AGU PUBLICATIONS

Geophysical Research Letters

Topographic Beta Spiral and Onshore Intrusion of the Kuroshio Current

De-Zhou Yang[1,2] (iD)**, Rui Xin Huang[3]** (iD)**, Bao-shu Yin[1,2,4]** (iD)**, Xing-Ru Feng[1]** (iD)**, Hai-ying Chen[1]**, **Ji-Feng Qi[1], Ling-jing Xu[1,4], Yun-long Shi[1,5], Xuan Cui[1,4], Guan-Dong Gao[1],** and **Jessica A. Benthuysen[6]** (iD)

[1]Key Laboratory of Ocean Circulation and Waves, Institute of Oceanology, Chinese Academy of Sciences, Qingdao, China, [2]Qingdao National Laboratory for Marine Science and Technology, Qingdao, China, [3]Department of Physical Oceanography, Woods Hole Oceanographic Institution, Woods Hole, MA, USA, [4]Department of Physical Oceanography, University of Chinese Academy of Sciences, Beijing, China, [5]School of Marine Sciences, Nanjing University of Information Science and Technology, Nanjing, China, [6]Australian Institute of Marine Science, Townsville, Queensland, Australia

Abstract The Kuroshio intrusion plays a vitally important role in carrying nutrients to marginal seas. However, the key mechanism leading to the Kuroshio intrusion remains unclear. In this study we postulate a mechanism: when the Kuroshio runs onto steep topography northeast of Taiwan, the strong inertia gives rise to upwelling over topography, leading to a left-hand spiral in the stratified ocean. This is called the topographic beta spiral, which is a major player regulating the Kuroshio intrusion; this spiral can be inferred from hydrographic surveys. In the world oceans, the topographic beta spirals can be induced by upwelling generated by strong currents running onto steep topography. This is a vital mechanism regulating onshore intruding flow and the cross-shelf transport of energy and nutrients from the Kuroshio Current to the East China Sea. This topographic beta spiral reveals a long-term missing link between the oceanic general circulation theory and shelf dynamic theory.

Plain Language Summary The water and material exchange between global ocean and marginal sea is attracting immense research interest because it significantly influences the coastal hydrodynamic environment and ecosystem. We first report the topographic beta spiral inferred from observations, which is generated by strong upwelling induced when strong western boundary current runs onto steep topography in coastal sea. We postulate that this mechanism plays a vital role in regulating intrusion/bifurcation of western boundary currents. This mechanism may be at work in many places in the world oceans; thus, it can be used as a clue in predicting the intrusion path and the bifurcation pattern of strong boundary currents. Similar to Ekman spiral, topographic beta spiral is one kind of very important and common spirals in the world oceans. In some cases, topographic beta spiral suggests that the intruding water mass originates from the deep water of western boundary current rather than surface water. Since temperature, oxygen and nutrients in the deep water are significantly different to the shelf water, this intruding water can influence coastal ecosystem and hypoxia.

1. Introduction

In the subtropical North Pacific Ocean the balance between the Ekman pumping and the planetary-vorticity gradient gives rise to the equatorward flow in the ocean interior, which is compensated by an intensified western boundary current, the Kuroshio Current, whose pathway in the East China Sea (ECS) is constrained by the continental slope of the ECS. The intrusion of the Kuroshio into the ECS plays an important role in the ocean circulation system over the ECS shelf, because the Kuroshio water is warm, salty, and rich in phosphate in the deep water. It has been reported that the intrusion of the Kuroshio mainly occurs northeast of Taiwan (Guo et al., 2006; Hsueh et al., 1992; Qiu & Imasato, 1990; Tang et al., 1999; Wu et al., 2017; Yang et al., 2011). Yang et al. proposed that there were two branches of the Kuroshio in the lower layer of the ECS in summer: a nearshore Kuroshio branch current (NKBC) and an offshore Kuroshio branch current (OKBC) (Yang et al., 2012).

The mechanism of the Kuroshio intrusion has been extensively investigated. The meeting of the Kuroshio with the zonally running shelf break northeast of Taiwan in the summer (the 200 m isobath in Figure 1 reflects the location of the shelf break) is an important factor for the onshore intrusion of the Kuroshio (Hsueh et al.,
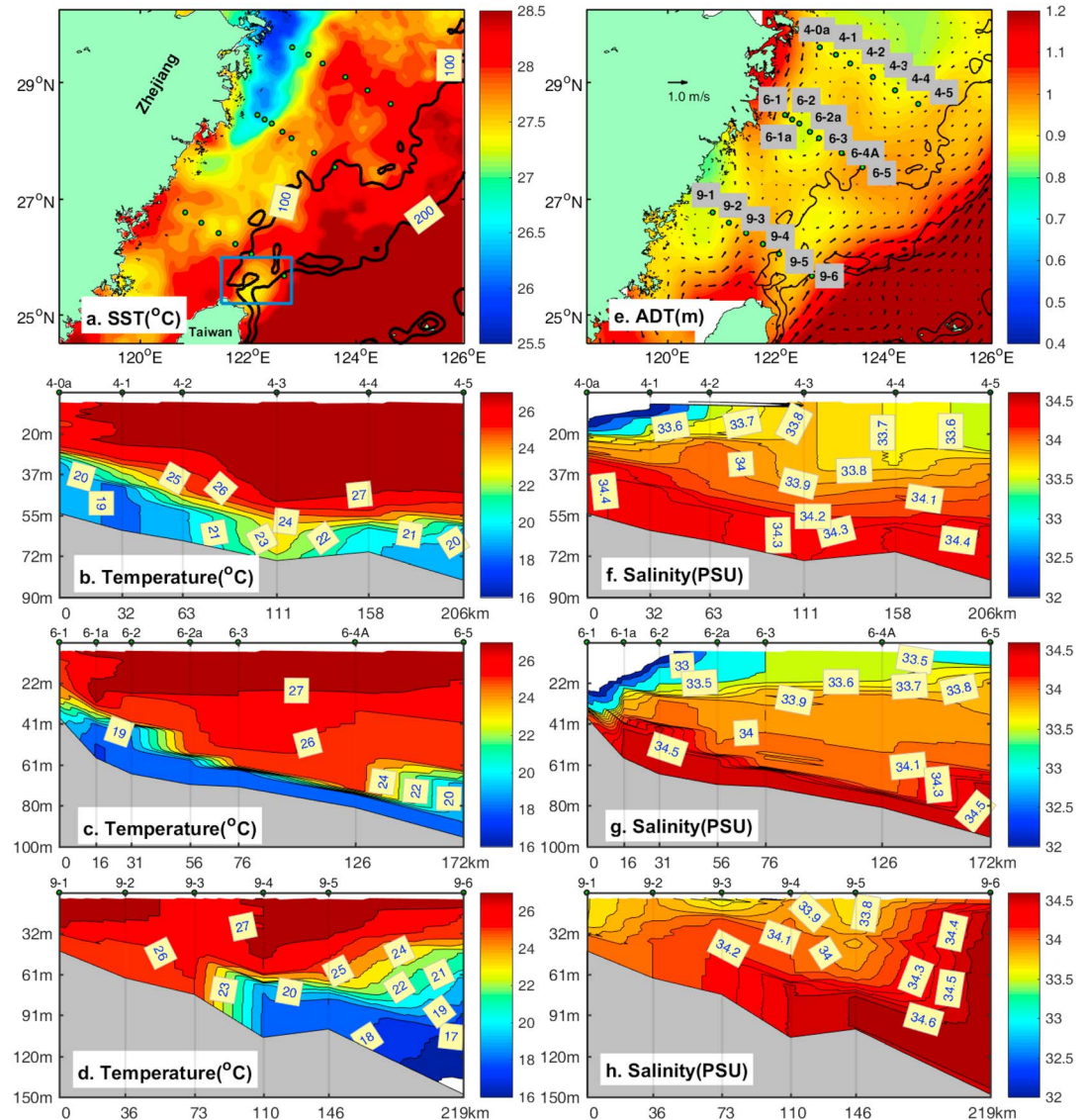
Figure 1. The Kuroshio intrusion inferred from hydrographic data. (a) The 10 day mean sea surface temperature (SST) (Maturi et al., 2014) corresponding to the cruise period from 29 August to 7 September 2015; (e) The absolute dynamic topography (ADT) and geostrophic current averaged over the same period, where the numbers indicate the station locations. (b–d) Observed temperature and (f–h) salinity.

1992; Hsueh et al., 1993; Tang et al., 2000). The planetary β effect and Taiwan Island are thought to be the main driving factors for the Kuroshio branch current (KBC) northeast of Taiwan (Qiu & Imasato, 1990).Using an idealized one-layer model (Hsueh et al., 1992) and a two-layer model (Hsueh et al., 1993), a formula for the intrusion angle of the KBC was postulated. It is also theorized that the seasonal variation of the onshore flux of the Kuroshio is mainly modulated by the Ekman transport, the seasonal variation of the Kuroshio mainstream, and the joint effect of the baroclinicity and relief term (Guo et al., 2006; Jacobs et al., 2000; Wu et al., 2014). Oey et al. (2010) concluded that winter cooling alone could cause a great northward intrusion of KBC onto the ECS shelf. It was reported that the Kuroshio intrusion can be partly attributed to vortex stretching of the intruded water column over topography (Yang et al., 2012) and to the westward impingement of eddies from the open ocean on the Kuroshio mainstream (Wu et al., 2017; Yin et al., 2017). The vertical structure of the Kuroshio intrusion was also inferred from the paths of major currents north of Taiwan (Yang et al., 2012); as shown in their Figure 14, the Kuroshio turns cyclonically from the surface to the bottom when it intrudes

onto the ECS shelf (Yang et al., 2012). In fact, it was reported that the KBC turns gradually to the west with increasing depth (Tang et al., 1999; Wong et al., 2000).

Despite recent progress, the driving mechanism of the NKBC intruding farther shoreward onto the ECS shelf compared with the OKBC remains to be investigated. Here we suggest a topographic beta spiral that can explain the vertical structure of the Kuroshio branches northeast of Taiwan and interpret the observed characteristics of the Kuroshio subsurface water on the ECS shelf that previous theory could not explain.

2. Observed Kuroshio Intrusions on the ECS Shelf

Recent cruise data from the ECS, collected by the Institute of Oceanology, Chinese Academy of Sciences (IOCAS) from 26 August to 2 September 2015, were used to examine the structure of the Kuroshio intrusion. Temperature and salinity were collected at each station, using the shipboard SBE 911 plus conductivity-temperature-depth (CTD) sensor manufactured by Sea-Bird.

Two cold and salty cores can be clearly seen in Figures 1b and 1f, and the nearshore core is 1° colder than the offshore core. This phenomenon is also evident in Figures 1c and 1g, although it is not as clear as that in Figures 1b and 1f. This feature has been previously identified in summer 2009 (Yang et al., 2012). In addition, it can also be easily identified in Figure 3 in Katoh et al. (2000), where the bottom water is colder in the shallow nearshore area than in the deep offshore area, see stations A1–A19 in their Figure 3. Therefore, this phenomenon is a relatively steady and common feature of the Kuroshio intrusion. Furthermore, in transects farther northward, these two cores were more clearly separated from each other (Figures 1b–1d and 1f–1h).

3. Theory

Large-scale motions in the ocean satisfy the geostrophic and hydrostatic approximations; the general form of density balance in a steady state is

$$u\rho_x + v\rho_y + w\rho_z = A_H\nabla^2\rho + A_V\rho_{zz} - \alpha\dot{q}/c_p, \tag{1}$$

where u, v, and w are current components in x, y, and z directions in Cartesian coordinates, ρ is the density, α the thermal expansion coefficient, $\dot{q}$ the rate of heating per unit mass, c_p the specific heat at constant pressure, and A_H and A_V the horizontal and vertical thermal diffusivities. The velocity angle is defined as $\theta = \tan^{-1}(v/u)$. Taking the derivative with respect to z and using the density balance and thermal wind relation lead to a relation (see the equation 2.232 in Huang, 2010):

$$\frac{d\theta}{dz} = \frac{\gamma}{u^2+v^2}\left[w\rho_z + \alpha\dot{q}/c_p + A_H\zeta_z/\gamma - A_V\rho_{zz}\right], \gamma = \frac{g}{f\rho_0}, \tag{2}$$

where g gravitational acceleration, f the Coriolis parameter, ρ_0 the reference density, and ζ_z the vertical component of the relative vorticity. This equation contains the vertical velocity and stratification term, cooling term, and the horizontal/vertical diffusion terms. Schott and Stommel (1978) first developed the theory of beta spiral; their basic equation (1.4) includes the first two terms in equation (2). If diffusion and cooling terms are negligible, we obtain

$$\frac{\partial\theta}{\partial z} = \frac{\gamma}{|\mathbf{u}_h|^2}w\frac{\partial\rho}{\partial z}, \mathbf{u}_h = \boldsymbol{u} + \boldsymbol{v}. \tag{3}$$

According to equation (3), the horizontal current rotation with depth is regulated by the vertical velocity and stratification; this is an important diagnostic relation for the beta spiral in the ocean, which is identical to equation 2.233 of Huang (2010) and equation 6.20.29 of Pedlosky (1986). The most important implication of this equation is that in the stratified ocean interior water column compression/stretching should lead to the rotation of the horizontal velocity vector.

In the wind-driven gyre interior the basic vorticity balance is $\beta v = f\partial w/\partial z$. Thus, the compression of the water column induced by Ekman pumping gives rise to horizontal advection due to the planetary vorticity gradient term β; the compression of water column also leads to the rotation of the horizontal velocity vector in the stratified ocean, and thus the name of the β spiral. For example, a β spiral in the mid-ocean of Northern Pacific Ocean is generated by the negative wind stress over the Pacific Ocean due to the midlatitude atmospheric westerly winds and trade winds in the equatorial regions.
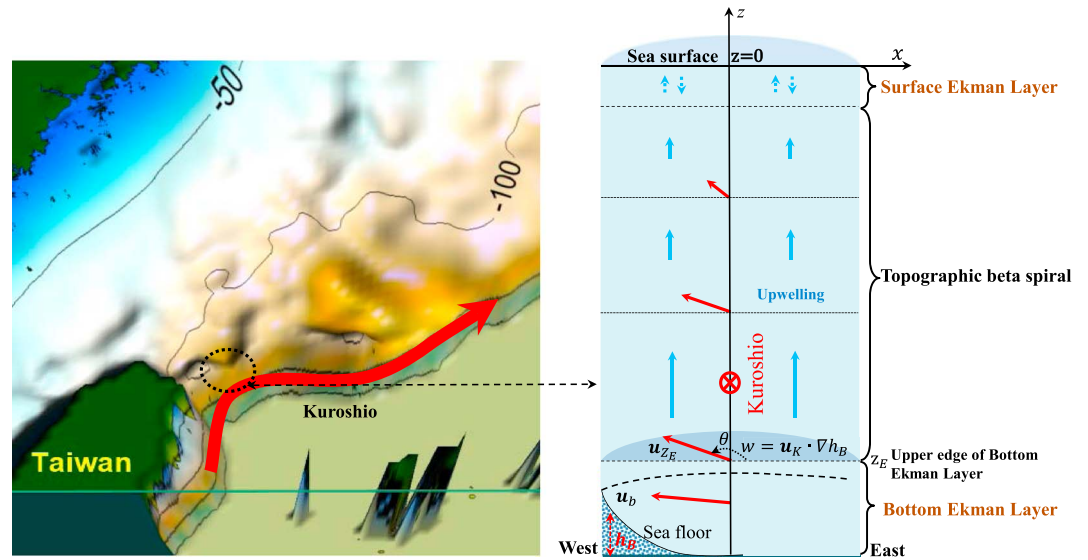
Figure 2. Sketch of the topographic beta spiral. (left) Topography and the Kuroshio mainstream. (right) Sketch of the topographic beta spiral. $\boldsymbol{u}_K$ denotes the horizontal velocity in the ocean interior above the bottom boundary; $\boldsymbol{u}_b$ indicates onshore flow in the bottom Ekman layer; z_E is the upper edge of the bottom Ekman layer, and $\boldsymbol{u}_{z_E}$ is the horizontal current vector at z_E.

In coastal areas, the strong boundary current moves on or offshore of the shelf break and can lead to the upwelling/downwelling near this area; this provides the vertical velocity required for generating the spiral. In recognizing the connection with the pioneering work of Schott and Stommel (1978) and Stommel and Schott (1977), we name this velocity structure the "topographic beta spiral."

Note that on the continental shelf, there is a strong Ekman layer in the bottom water (Figure 2), which is, however, negligible in the mid-ocean because the deep water is usually considered as motionless. In fact, equation (3) omits the contribution due to friction in the boundary layers. As a result, equation (3) is only applicable to the middle water column away from the Ekman layers on the surface and bottom, where the horizontal current vectors are strongly affected by friction. On the ECS shelf the average thickness of bottom Ekman layer at 200 m isobaths is ~18 m (Zhang et al., 2017). Between these two boundary Ekman layers, the horizontal velocity vector should rotate with depth according to equation (3).

4. Application of the Theory in the ECS

As shown by sea surface temperature (SST) in the area inside a small blue box in Figure 1a, cold surface water is frequently found northeast of Taiwan and this area is an important upwelling domain (Tang et al., 2000). Regional Ocean Modeling System (ROMS) (Shchepetkin & McWilliams, 2005) has been successfully used to simulate the ocean current in the ECS, yielding good agreement with observations (Yang et al., 2012). The localized upwelling has been successfully reproduced by the model results. Figure 3a shows that there is a strong upwelling area near the meeting point between the Kuroshio and the shelf break. Therefore, the numerical output is used to examine the driving mechanism of the upwelling.

The dominating factors at the meeting points can be identified from the meridional momentum equation:

$$\underbrace{\frac{\partial V}{\partial t}}_{V_{accel}} + \underbrace{\mathbf{U}\cdot\nabla V}_{V_{hadv}} + \underbrace{fU}_{V_{cor}} + \underbrace{\frac{1}{\rho_0}\frac{\partial P}{\partial y}}_{V_{prsgrd}} - \underbrace{D_V}_{V_{hvisc}} + U_{sstr} + U_{bstr} = 0, \tag{4}$$

where **U** is the vertically averaged horizontal current, V is the vertically averaged meridional velocity, and P is pressure. In equation (3), the first term is the local acceleration, the second term is the advection term (the inertial term), the third term is Coriolis term, the fourth term is the pressure gradient, V_{hvisc} is horizontal viscosity term, and U_{sstr} and U_{bstr} denote surface stress (surface friction) and bottom stress (bottom friction). As
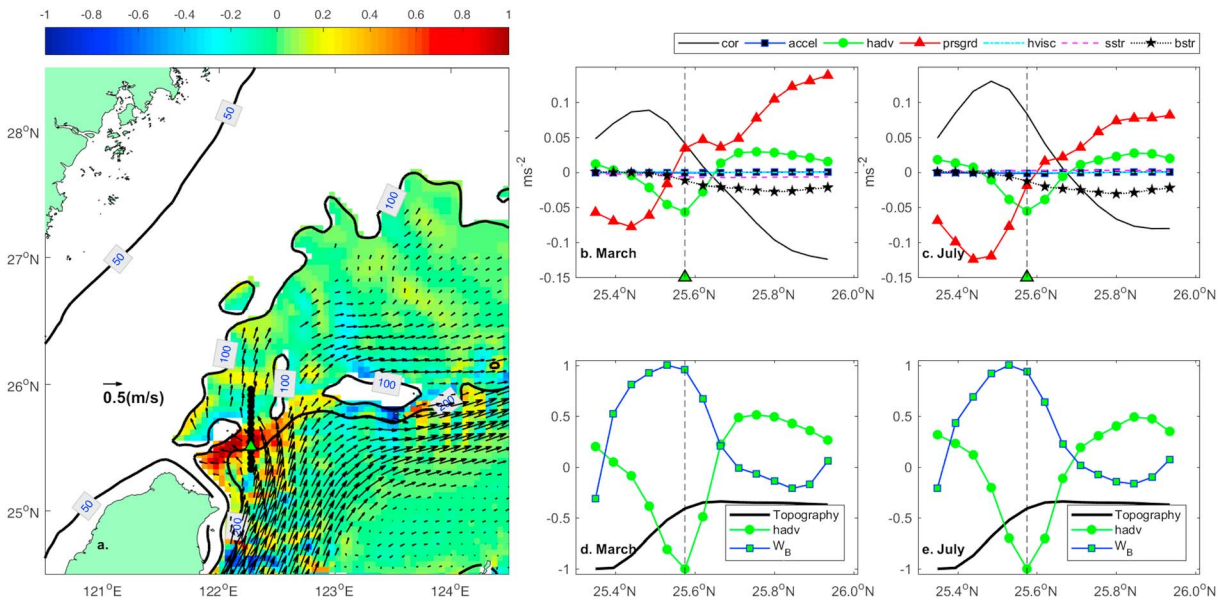
Figure 3. Velocity distribution and momentum balance for a cross-shelf transect. (a) Monthly mean vertical velocity (color map, in unit of 10^{-3} ms^{-1}) and horizontal current (vector, in unit of ms^{-1}) at the depth of 100 m in July, overlaid with 50 m, 100 m, and 200 m isobaths; (b and c) the distributions of each term in equation (4) along a meridional transect (dotted line in Figure 3a) in March and July;(d and e) topography, inertial term, and topographic upwelling (all normalized by their maximum) along the same transect and time as in Figures 3b and 3c.

shown in Figures 3b and 3c, most of the cross-shelf flow is geostrophic, that is, the Coriolis term is mainly balanced by the pressure gradient term. However, near the collision point (the triangle in Figure 3a) the inertia term associated with the northward flowing Kuroshio becomes one of the dominating terms in the momentum balance. As shown in Figures 3d and 3e, strong upwelling is closely linked to the strong inertia of northward flowing Kuroshio when it abruptly meets with the zonally running shelf break.

The vertical velocity above the Ekman layer over a sloping bottom contains two terms (Pedlosky, 1986)

$$w_B = \boldsymbol{u}_K \cdot \nabla h_B + \zeta \sqrt{E_V}/2, \tag{5}$$

where $\boldsymbol{u}_K$ indicates the horizontal velocity in the ocean interior above the bottom boundary layer, E_V is the vertical Ekman number, and ζ represents a variable associated with relative vorticity immediately outside the Ekman boundary layer. According to the momentum equation balance shown in Figure 3, the last term in equation (5) is negligible relative to the topography term near a steep shelf break. The vertical velocity above the bottom Ekman layer is a function of vertical velocity at the upper edge of the bottom Ekman layer (see z_E in Figure 2). For simplicity, we assume that the vertical velocity for the water column between the Ekman layers on the sea surface and seafloor has a linear profile

$$w(z) = \frac{|z|}{H} \boldsymbol{u}_K \cdot \nabla h_B, \tag{6}$$

where H is the thickness of water column, omitting the boundary layers. As shown in the Figure 4, equation (6) gives a qualitatively reasonable estimation of the w in the water column between the top and bottom Ekman layers. Thus, we have

$$\frac{\partial \theta}{\partial z} = \frac{|z|}{H} \frac{(\boldsymbol{u}_K \cdot \nabla h_B) g}{f_0 \rho_0 |\mathbf{u}_h|^2} \frac{\partial \rho}{\partial z}, z > z_E. \tag{7}$$

Equation (7) suggests that the intrusion from the strong deep current onto the shelf can lead to a spiral structure. In general, for large-scale steady flow the ocean is stably stratified, so that $\partial \rho / \partial z$ is negative. Equation (7) therefore implies three types of vertical structure of horizontal current vectors corresponding to three types of topography.

In case one, where $\boldsymbol{u}_K \cdot \nabla h_B = 0$, the ocean currents flow along the isobaths of topography; so that there is no rotation of velocity vector, that is, no Kuroshio intrusion.

In case two, where $\boldsymbol{u}_K \cdot \nabla h_B < 0$, the bottom water flows down the slope of topography and downwelling occurs. According to equation (7), $\partial\theta/\partial z > 0$; thus, the surface part of the Kuroshio is more shoreward than the subsurface water. As a result, the onshore cross-shelf intrusion of the Kuroshio is mainly confined to the upper layers.

In case three where $\boldsymbol{u}_K \cdot \nabla h_B > 0$, so that $\partial\theta/\partial z < 0$. This case represents the situation northeast of Taiwan, where the Kuroshio continues its northward flow as shown in Figure 2. Due to the sudden change in the orientation of topography, the current runs almost perpendicular to the isobaths. Within the bottom Ekman layer, the horizontal current rotates in the form of left-hand spiral (Figure 2) due to bottom friction. At the upper edge of bottom Ekman layer, the change of $\boldsymbol{u}_K$ due to topography induces strong upwelling according to equation (5). Thus, the horizontal velocity vector above z_E is in the form of a left-hand spiral, that is, the horizontal flow continuously turns anticyclonically with increasing z relative to $\boldsymbol{u}_{z_E}$. As a result, the Kuroshio subsurface water intrudes farther westward than the Kuroshio surface water, as shown in Figure 2. In this case, onshore cross-shelf intrusion of the Kuroshio is mainly confined to the deep layers. In northeast coast area of Taiwan, the characteristic values are the following: $\partial\rho/\partial z = O(0.03 \text{ kgm}^{-4})$, $\boldsymbol{u}_K \cdot \nabla h_B = O(0.005 \text{ms}^{-1})$, $\gamma = O(100 \ m^4 \text{ kg}^{-1} \text{ s}^{-1})$, and $|\boldsymbol{u}_h| = O(1 \text{ ms}^{-1})$. Hence, the angle between the surface and bottom current vectors is approximately $60°$.

The ROMS model output was used to verify this mechanism. The model forced by climatological data (heat flux, water flux, momentum flux, Changjiang River flux, and 10 tidal components) was run for 6 years for spin-up. Then, the spin-up ocean state of the climatology run at the sixth model year was used as initial conditions for float experiments. The model is configured in the same way as in Yang et al. (2012). According to equation (7), the horizontal flow should be a left-hand spiral. As shown in Figure 4a, at the conjuncture of the Kuroshio and the continental shelf deep floats trajectories are more shoreward than shallow floats; thus, the cold water in deep layers should intrude farther shoreward than water in the upper layers. The patterns of flow trajectory are consistent with the two salty and cold bottom cores inferred from observations shown in Figure 1, where the temperature of the nearshore core was 1° colder than the offshore core, although the offshore core was located in water deeper than the nearshore core.

Thus, the observed vertical structure of KBC, OKBC, and NKBC in the ECS can be explained by this mechanism, as shown in Figure 4a. Furthermore, the horizontal velocity profiles in the surface Ekman layer are different. In March, it appears as a well-defined right-hand spiral, but in July it appears as a vaguely defined left-hand spiral. Such a difference is due to the fact that the monsoon reverses its direction from March to July. The vertical turning with depth in the whole water column is composed of three segments: a spiral in the surface Ekman layer, where the sense of rotation varies with season, a left-hand spiral in the bottom Ekman layer, and a left-hand topographic beta spiral between these two Ekman layers as shown in the Figures 2 and 4.

Based on the direct output from the model, the monthly mean w at the meeting point in March and July is plotted in Figures 4c and 4d. Equation (3) can be used to infer the vertical velocity from stratification and the rotation of the horizontal velocity vector, whose values can be diagnosed from the model output. It is interesting to note that the w profiles calculated from equations (3) and (6) qualitatively agree with model results, especially in July, as shown in Figure 4d. The angle θ has been directly calculated from the modeled horizontal current; the beautiful spirals obtained are shown in Figures 4e and 4f. According to the theory, the horizontal flow turns clockwise with increasing z relative to the bottom current. At the depth of 20 m, the horizontal velocity vector rotates about 60° clockwise relative to the bottom vector. In the surface layer, the sense of rotation changes obviously from March to July, and this is attributed to the variation of monsoon winds. Below the surface Ekman layer, the variation in the spiral from March to July comes from the seasonal variation in the Kuroshio (Wu et al., 2014), which could change the upwelling near the bottom according to the equation (7). Therefore, the meeting location of the Kuroshio with the shelf break as well as the angle between the Kuroshio and the topography gradient changes from winter to summer. Thus, the intrusion branches should likewise spin differently according to the equation (7). Moreover, Figures 4e and 4f show a good agreement between the equation (7) and model results. Thus, equation (7) provides a convenient way to estimate the spiral at the meeting point whenever a strong current is not parallel to the isobaths.

According to equation (7), if the northward flowing Kuroshio is more perpendicular to the isobaths, the rotation of the left-hand spiral is stronger. Furthermore, equation (7) shows that the rotation of the ocean current is inversely proportional to the speed of the current and the Coriolis parameter; thus, topographic beta spiral
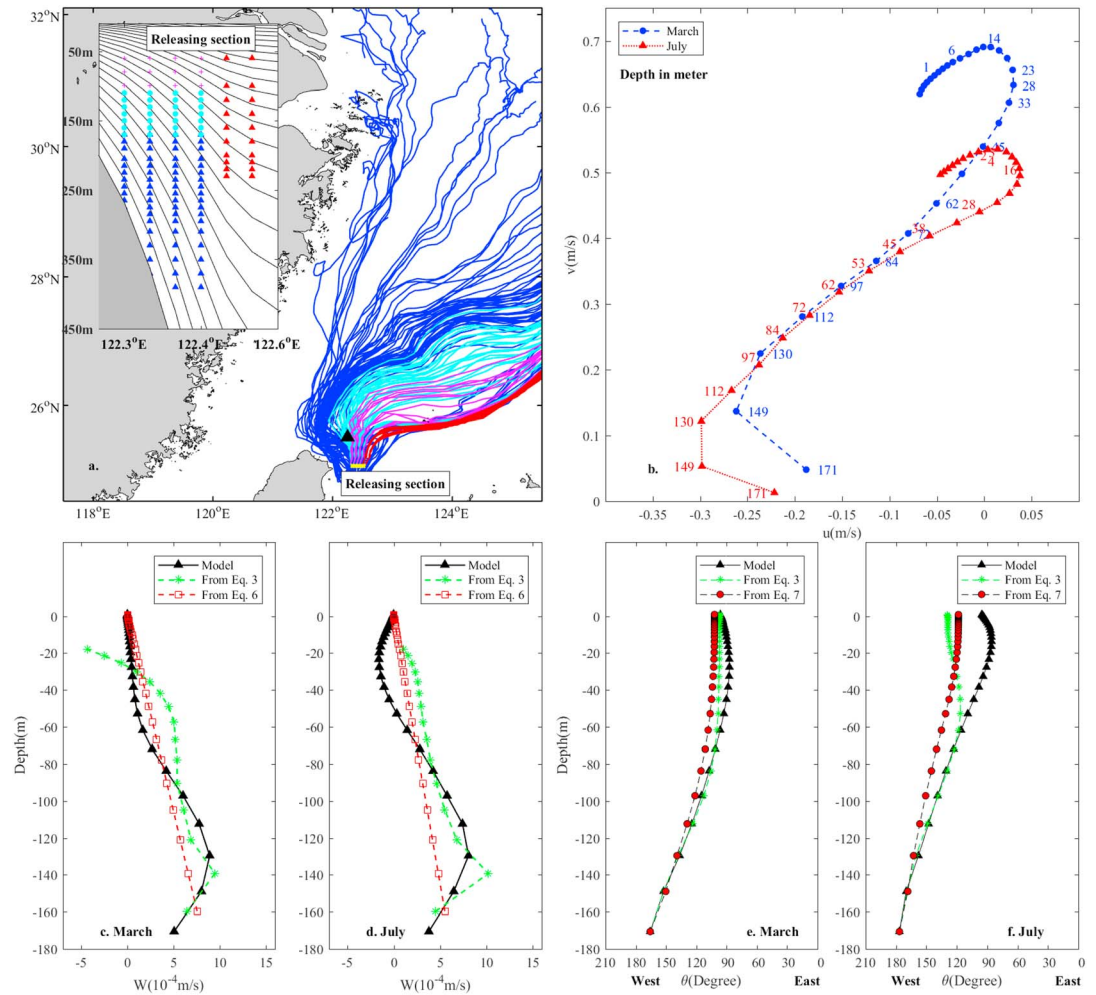
Figure 4. Topographic beta spiral. (a) Float trajectories from numerical experiments of the climatology run from 1 March to 1 September, where the floats were released along a transect (details shown in the insert) on 1 March; (b) the spiral of the horizontal current; (c and d) profiles of w from model output, calculated from equations (3) and (6) at a meeting point (the triangle in Figure 4a) in March and July, respectively; and (e and f) θ profiles calculated from the modeled horizontal current, equations (3) and (7) in March and July, respectively.

may be more pronounced for relatively weak current at lower latitudes. On the other hand, the rotation is proportional to the stratification; in other words, the seasonal variation of the Kuroshio intrusion in the deep water is partially due to seasonal difference in stratification.

Figure 5 shows that the strongest bottom upwelling occurs northeast of Taiwan, where the cross-stream onshore intrusion reaches the peak value as high as ~1.2 sverdrup (Sv) (1 Sv ≡ 10^6 m^3 s^{-1}). It has been reported that there is a cross-shelf intrusion of 1.4 Sv originating from the Kuroshio (Isobe, 2008) on the ECS shelf. Therefore, the intrusion identified here is the most important source of the cross-shelf exchange, and the topographic beta spiral may be a key dynamical factor regulating the onshore intrusion of the Kuroshio. According to equation (7), there is onshore/offshore cross-shelf intrusion along the shelf break wherever the Kuroshio is not parallel to the isobaths. This prediction is clearly demonstrated by the close correlation between intrusion flux and bottom upwelling in Figures 5b and 5c. The w_B term can be further separated into the cross-stream and along-stream terms (see $\boldsymbol{n}$ and $\boldsymbol{t}$ in Figure 5a for the orientation).

$$w_B = \boldsymbol{u}_K \cdot \nabla h_B = \underbrace{u_n \operatorname{grad}(h_B)_n}_{w_{Bn}} + \underbrace{u_t \operatorname{grad}(h_B)_t}_{w_{Bt}}. \tag{8}$$

The stronger intrusion involves a nonlinear topography-induced upwelling. If there is no along-stream topography, the gradient term vanishes, $w_{Bt} = 0$; so that there is no upwelling, and no topographic beta spiral;
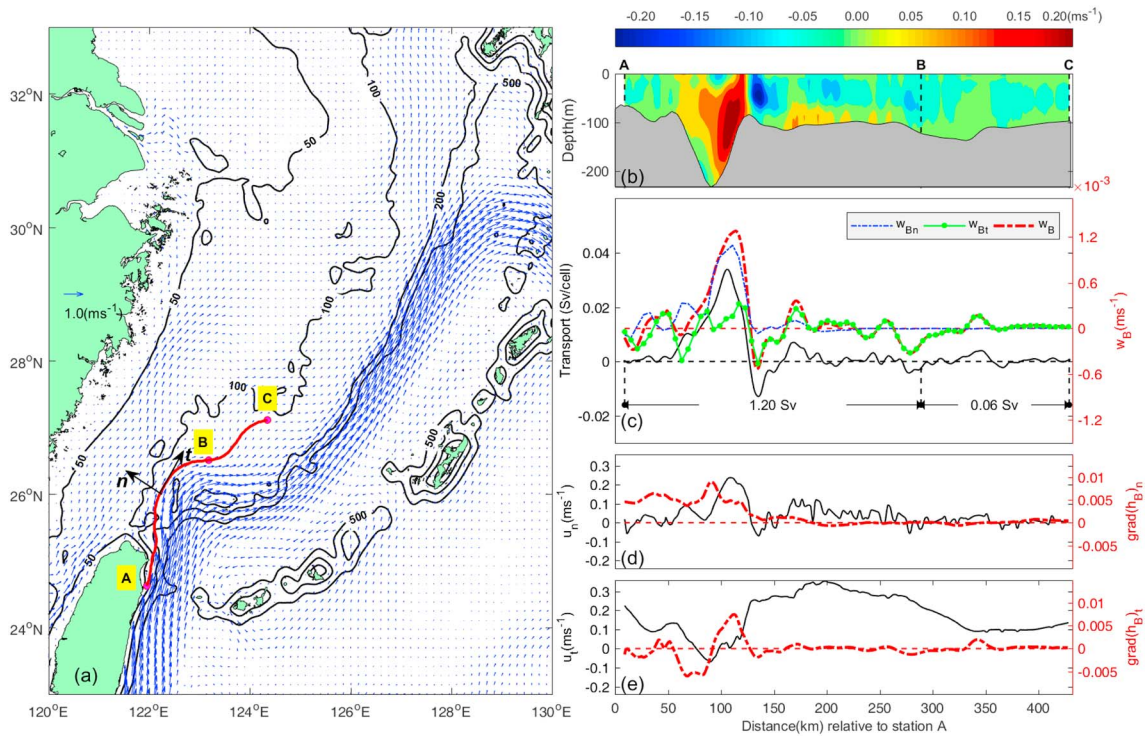
Figure 5. Cross-shelf intrusion and topographic upwelling during the warm season (from March to July). (a) Horizontal surface current, overlaid with 50 m, 100 m, and 200 m isobaths, where the line ABC represents the inshore edge of the Kuroshio Current defined by the 0.9 m sea surface height contour, n is the unit vector normal to the line ABC and t is the unit vector tangent to the line ABC; (b) normal velocity perpendicular to the ABC line; (c) the corresponding cross-stream volume flux integrated over the whole water column between two grid points (the distance between each pair of grid is 1 km) along the ABC line where w_B calculated from equation (5), and w_{Bn} and w_{Bt} calculated from equation (8); (d and e) the cross-stream and along-stream components of $\boldsymbol{u}_K$ and ∇h_B.

consequently, $u_n = 0$, $w_{Bn} = 0$, that is, no onshore intrusion. If there is along-stream topography, flow runs onto the topography, creating an upwelling $w_{Bt} > 0$. This upwelling induces the topography beta spiral, and thus an onshore intrusion velocity $u_n > 0$. As a result, there is additional upwelling associated with the onshore flow. This leads to enhanced topographic spiral and more onshore flow and even stronger upwelling. In this way, the nonlinear topography-induced upwelling in the relatively confined region of the Kuroshio Current combined with the basin scale dynamics gives rise to a complicated solution, which is consistent with both the global and local dynamical balances. It is important to emphasize that the structure of the topographic spiral and the pathway of the intruded water masses is set not only by the local dynamics but also the basin-scale dynamics.

The topographic beta spiral described above plays key roles in the coastal environment because it leads to a strong intrusion onto the continental shelf carrying large amounts of material from the deep water. In the ECS, the shoreward intruding cold, oxygen-poor, and phosphate-rich deep water sometimes can reach as far as the Zhoushan fishery ground (a famous fishery ground in Asia and an upwelling area) off the coasts of Zhejiang (see Figure 1a) (Yang et al., 2013), where hypoxia, harmful algal blooms, and jellyfish blooms are frequently reported (Wang & Wu, 2009; Zhou et al., 2008; Zhu et al., 2011). Thus, topographic beta spiral is a vitally important mechanism involved in the interaction between the open ocean and coastal ocean.

5. Conclusion

The Kuroshio bifurcation or intrusion has been discussed in many previous studies. Recent in situ observations and numerical float experiments clearly demonstrated the left-hand spiral structure of the currents northeast of Taiwan. Our analysis shows that such a left-hand spiral can be explained in simple dynamical language as follows.

In the ocean interior, the essential ingredients of the beta spiral are the stratification and vertical velocity, as shown in equation (3). Northeast of Taiwan, the strong Kuroshio runs almost perpendicular to the nearly zonal shelf break; thus, large inertial term induces strong upwelling in the conjunction area. In the stratified ocean, this topographically induced upwelling gives rise to the topographic beta spiral.

This left-hand spiral leads to the onshore movement of the Kuroshio water in deep layers, which is cold and rich in phosphate. Thus, the topographic beta spiral is one of the major mechanisms regulating the Kuroshio intrusion. The contribution associated with the topographic beta spiral to the total transport of the Kuroshio intrusion and other forms of currents bifurcated from the Kuroshio are an important issue to be explored in further studies.

The topographic beta spiral may exist in many places in the world oceans wherever a strong current is not parallel to the isobaths. An important by-product of such topographic spiral is the rotation and bifurcation of the current or some kind of on-shore intrusion or offshore currents. The topographic beta spiral provides a dynamical channel to bring the cold, oxygen-poor, and nutrient-rich deep water from the strong current to the continental shelf. Therefore, the topographic beta spiral reveals a long-term missing link between the oceanic general circulation theory and shelf dynamic theory, and it is important for understanding the links between changes in ocean climate, coastal hypoxia, and ecological perturbations.

References

Guo, X. Y., Miyazawa, Y., & Yamagata, T. (2006). The Kuroshio onshore intrusion along the shelf break of the East China Sea: The origin of the Tsushima Warm Current. *Journal of Physical Oceanography*, *36*(12), 2205–2231. https://doi.org/10.1175/JPO2976.1

Hsueh, Y., Chern, C. S., & Wang, J. (1993). Blocking of the Kuroshio by the continental-shelf northeast of Taiwan. *Journal of Geophysical Research*, *98*(C7), 12,351–12,359. https://doi.org/10.1029/93JC01075

Hsueh, Y., Wang, J., & Chern, C. S. (1992). The intrusion of the Kuroshio across the continental-shelf northeast of Taiwan. *Journal of Geophysical Research*, *97*(C9), 14,323–14,330. https://doi.org/10.1029/92JC01401

Huang, R. X. (2010). *Ocean circulation: Wind-driven and thermohaline processes* (pp. 3302–3305). New York: Cambridge University Press.

Isobe, A. (2008). Recent advances in ocean-circulation research on the Yellow Sea and East China Sea shelves. *Journal of Oceanography*, *64*(4), 569–584. https://doi.org/10.1007/s10872-008-0048-7

Jacobs, G. A., Hur, H. B., & Riedlinger, S. K. (2000). Yellow and East China Seas response to winds and currents. *Journal of Geophysical Research*, *105*(C9), 21,947–21,968. https://doi.org/10.1029/2000JC900093

Katoh, O., Morinaga, K., & Nakagawa, N. (2000). Current distributions in the southern East China Sea in summer. *Journal of Geophysical Research*, *105*(C4), 8565–8573. https://doi.org/10.1029/1999JC900309

Maturi, E., Sapper, J., Harris, A., & Mittaz, J. (2014). GHRSST level 4 OSPO global foundation sea surface temperature analysis (GDS version 2). *National Oceanographic Data Center, NOAA, Dataset*. https://doi.org/10.7289/V5SQ8XFH

Oey, L. Y., Hsin, Y. C., & Wu, C. R. (2010). Why does the Kuroshio northeast of Taiwan shift shelfward in winter? *Ocean Dynamics*, *60*(2), 413–426. https://doi.org/10.1007/s10236-009-0259-5

Pedlosky, J. (1986). *Geophysical fluid dynamics*. New York: Springer-Verlag.

Qiu, B., & Imasato, N. (1990). A numerical study on the formation of the Kuroshio counter current and the Kuroshio branch current in the East China Sea. *Continental Shelf Research*, *10*(2), 165–184. https://doi.org/10.1016/0278-4343(90)90028-K

Schott, F., & Stommel, H. (1978). Beta spirals and absolute velocities in different oceans. *Deep Sea Research*, *25*(11), 961–1010. https://doi.org/10.1016/0146-6291(78)90583-0

Shchepetkin, A. F., & McWilliams, J. C. (2005). The regional oceanic modeling system (ROMS): A split-explicit, free-surface, topography-following-coordinate oceanic model. *Ocean Model*, *9*(4), 347–404. https://doi.org/10.1016/j.ocemod.2004.08.002

Stommel, H., & Schott, F. (1977). The beta spiral and the determination of absolute velocity-field from hydrographic station data. *Deep-Sea Research*, *24*(3), 325–329. https://doi.org/10.1016/0146-6291(77)93000-4

Tang, T. Y., Hsueh, Y., Yang, Y. J., & Ma, J. C. (1999). Continental slope flow northeast of Taiwan. *Journal of Physical Oceanography*, *29*(6), 1353–1362. https://doi.org/10.1175/1520-0485(1999)029%3C1353:CSFNOT%3E2.0.CO;2

Tang, T. Y., Tai, J. H., & Yang, Y. J. (2000). The flow pattern north of Taiwan and the migration of the Kuroshio. *Continental Shelf Research*, *20*(4-5), 349–371. https://doi.org/10.1016/S0278-4343(99)00076-X

Wang, J. H., & Wu, J. Y. (2009). Occurrence and potential risks of harmful algal blooms in the East China Sea. *Science of the Total Environment*, *407*(13), 4012–4021. https://doi.org/10.1016/j.scitotenv.2009.02.040

Wong, G. T. F., Chao, S. Y., Li, Y. H., & Shiah, F. K. (2000). The Kuroshio edge exchange processes (KEEP) study—An introduction to hypotheses and highlights. *Continental Shelf Research*, *20*(4-5), 335–347. https://doi.org/10.1016/S0278-4343(99)00075-8

Wu, C. R., Hsin, Y. C., Chiang, T. L., Lin, Y. F., & Tsui, I. F. (2014). Seasonal and interannual changes of the Kuroshio intrusion onto the East China Sea Shelf. *Journal of Geophysical Research: Oceans*, *119*, 5039–5051. https://doi.org/10.1002/2013JC009748

Wu, C.-R., Wang, Y.-L., Lin, Y.-F., & Chao, S.-Y. (2017). Intrusion of the Kuroshio into the South and East China Seas. *Scientific Reports*, *7*(1), 7895. https://doi.org/10.1038/s41598-017-08206-4

Yang, D. Z., Yin, B. S., Liu, Z. L., Bai, T., Qi, J. F., & Chen, H. Y. (2012). Numerical study on the pattern and origins of Kuroshio branches in the bottom water of southern East China Sea in summer. *Journal of Geophysical Research*, *117*, C02014. https://doi.org/10.1029/2011JC007528

Yang, D. Z., Yin, B. S., Liu, Z. L., & Feng, X. R. (2011). Numerical study of the ocean circulation on the East China Sea shelf and a Kuroshio bottom branch northeast of Taiwan in summer. *Journal of Geophysical Research*, *116*, C05015. https://doi.org/10.1029/2010JC006777

Yang, D. Z., Yin, B. S., Sun, J. C., & Zhang, Y. (2013). Numerical study on the origins and the forcing mechanism of the phosphate in upwelling areas off the coast of Zhejiang province, China in summer. *Journal of Marine Systems*, *123-124*, 1–18, doi:https://doi.org/10.1016/j.jmarsys.2013.04.002

Yin, Y. Q., Lin, X. P., He, R. Y., & Hou, Y. J. (2017). Impact of mesoscale eddies on Kuroshio intrusion variability northeast of Taiwan. *Journal of Geophysical Research: Oceans*, *122*, 3021–3040. https://doi.org/10.1002/2016jc012263

Zhang, J., Guo, X. Y., Zhao, L., Miyazawa, Y., & Sun, Q. (2017). Water exchange across isobaths over the continental shelf of the East China Sea. *Journal of Physical Oceanography*, *47*(5), 1043–1060. https://doi.org/10.1175/Jpo-D-16-0231.1

Zhou, M. J., Shen, Z. L., & Yu, R. C. (2008). Responses of a coastal phytoplankton community to increased nutrient input from the Changjiang (Yangtze) River. *Continental Shelf Research*, *28*(12), 1483–1489. https://doi.org/10.1016/j.csr.2007.02.009

Zhu, Z. Y., Zhang, J., Wu, Y., Zhang, Y. Y., Lin, J., & Liu, S. M. (2011). Hypoxia off the Changjiang (Yangtze River) Estuary: Oxygen depletion and organic matter decomposition. *Marine Chemistry*, *125*(1–4), 108–116. https://doi.org/10.1016/j.marchem.2011.03.005